Multiple harmonic ULF waves in the plasma sheet boundary layer observed by Cluster

M. J. Engebretson,[1] C. R. G. Kahlstorf,[1] J. L. Posch,[1] A. Keiling,[2] A. P. Walsh,[3] R. E. Denton,[4] M. C. Broughton,[4] C. J. Owen,[3] K.-H. Fornaçon,[5] and H. Rème[6,7]

Received 13 July 2010; revised 7 September 2010; accepted 14 September 2010; published 10 December 2010.

[1] The passage of the Cluster satellites in a polar orbit through Earth's magnetotail has provided numerous observations of harmonically related Pc 1–2 ULF wave events, with the fundamental near the local proton cyclotron frequency Ω_{cp}. Broughton et al. (2008) reported observations by Cluster of three such events in the plasma sheet boundary layer, and used the wave telescope technique to determine that their wave vectors **k** were nearly perpendicular to **B**. This paper reports the results of a search for such waves throughout the 2003 Cluster tail passage. During the 4 month period of July–October 2003, 35 multiple-harmonic wave events were observed, all in the plasma sheet boundary layer (PSBL). From the first observed event (22 July) to the last (28 October), 13 of Cluster's 42 tail passes had at least one event. The wave events were rather evenly distributed from $X_{GSE} = -7$ R_E out to the Cluster apogee distance of −18 R_E, with one event observed at −4 R_E. Z_{GSE} for these events ranged from −10 to −3 R_E and +3 to +7 R_E (i.e., there were no events for $|Z| < 3$ R_E). The wave events, with durations from ~1 to 50 min, were consistently associated with signatures of the PSBL: elevated fluxes of counterstreaming ions with energies ranging from ~3 to 30 keV, and elevated fluxes of electrons with energies ranging from 0.25 to ~5 keV. Analysis of plasma parameters suggests that although waves occurred only when the ion beta exceeded 0.1 (somewhat larger than typical for the PSBL), ion particle pressure may be of more physical importance in controlling wave occurrence. Electron distributions were more isotropic in pitch angles than the ion distributions, but some evidence of counterstreaming electrons was detected in 83% of the events. The ions also showed clear signatures of shell-like or ring-like distributions; i.e., with reduced fluxes below the energy of maximum flux. The suprathermal ion fluxes were asymmetric in all events studied, with more ions streaming earthward (for events both north and south of the central plasma sheet). Good agreement between the observed frequency of the fundamental harmonic and the local Ω_{cp} suggests that the waves were observed near the region of their origin and did not propagate along **B**, consistent with the wave telescope analysis.

Citation: Engebretson, M. J., C. R. G. Kahlstorf, J. L. Posch, A. Keiling, A. P. Walsh, R. E. Denton, M. C. Broughton, C. J. Owen, K.-H. Fornaçon, and H. Rème (2010), Multiple harmonic ULF waves in the plasma sheet boundary layer observed by Cluster, *J. Geophys. Res.*, *115*, A12225, doi:10.1029/2010JA015929.

1. Introduction

[2] Multiple-harmonic electromagnetic waves in the ULF band have been reported occasionally since the early 1970s near the geomagnetic equator, and more recently in the plasma sheet boundary layer (PSBL) in Earth's magnetotail [see, e.g., *Broughton et al.*, 2008, and references therein]. The PSBL, which separates the dense plasma sheet from the much more rarified tail lobes, plays an important but not yet fully understood role in thermalizing ionospheric plasma that is energized and convected to Earth's magnetotail lobes as well as solar wind plasma entering on open field lines; both ultimately return earthward via the central plasma sheet (CPS).

[3] The PSBL is populated by electron and ion beams traveling parallel and antiparallel to the magnetic field directions [*Parks et al.*, 1984, 2001]. The transition between the highly anisotropic plasma distributions of the PSBL and

[1]Department of Physics, Augsburg College, Minneapolis, Minnesota, USA.
[2]Space Sciences Laboratory, University of California, Berkeley, California, USA.
[3]Mullard Space Science Laboratory, University College London, Dorking, UK.
[4]Department of Physics and Astronomy, Dartmouth College, Hanover, New Hampshire, USA.
[5]Institut für Geophysik und Extraterrestrische Physik, Technische Universität Braunschweig, Braunschweig, Germany.
[6]CESR, University of Toulouse, UPS, Toulouse, France.
[7]UMR 5187, CNRS, Toulouse, France.

0148-0227/10/2010JA015929

the much more isotropic plasma sheet is thought to be mediated by one or more wave-particle interaction processes. Waves that could isotropize this plasma, with frequencies near the local proton cyclotron frequency Ω_{cp}, have been observed in this region by several spacecraft [e.g., *Tsurutani and Smith*, 1984; *Tsurutani et al.*, 1985; *Angelopoulos et al.*, 1989; *Chaston et al.*, 1994, 2002; *Bauer et al.*, 1995; *Kawano et al.*, 1994; *Bogdanov et al.*, 2003].

[4] Recently, *Broughton et al.* [2008], using data from the four closely spaced Cluster spacecraft, reported three such events during late 2003 while Cluster traversed the PSBL, and used the wave telescope technique to find that the **k** vector of these waves was nearly perpendicular to **B**. We report here the results of a survey of the entire set of Cluster passes in Earth's magnetotail during 1 July to 1 November 2003, showing that these waves are a common feature of the PSBL. Section 2 describes the instruments used in this study, sections 3 and 4 show wave and suprathermal particle observations for two example events, and section 5 presents a statistical study of these wave events and the ion and electron distributions associated with them. The observations are discussed and summarized in section 6. A companion paper [*Denton et al.*, 2010] uses the Cluster observations during one of these events (9 September 2003) along with the WHAMP electromagnetic plasma wave dispersion code to analyze the instability of the observed plasma, and confirms that the ring-like character of the observed ion distributions can cause wave growth at Ω_{cp} and its harmonics.

2. Data Set

[5] The four spacecraft of the Cluster II mission were launched in late summer 2000 into a highly elliptical polar orbit with apogee of 19.6 R_E, perigee of 4 R_E, and 57 h period [*Escoubet et al.*, 2001]. The interspacecraft separation varied from 100 to 10000 km throughout the mission; during Cluster's tail passage in late 2003 the separations were often small enough (~100 km) to allow use of the wave telescope technique [*Motschmann et al.*, 1996; *Glassmeier et al.*, 2001]. The FGM instrument on each Cluster spacecraft [*Balogh et al.*, 2001] consists of redundant triaxial fluxgate magnetic field sensors on one of two radial booms; it measures the vector magnetic field magnitude and direction with a resolution up to 67 samples per second, and at 22.416 samples per second in nominal mode. The Cluster Ion Spectroscopy (CIS) experiment [*Rème et al.*, 2001] is composed of a time-of-flight Composition and Distribution Ion Function analyzer, CODIF, and a Hot Ion Analyzer, HIA, which can determine the energy, composition, and three-dimensional distributions of the major magnetospheric ions (H^+, He^+, He^{++} and O^+) in the energy range from 0 to 40 keV. The Plasma Electron and Current Experiment, PEACE [*Johnstone et al.*, 1997] can determine the energy and three-dimensional distributions of electrons with energies from about 0.7 eV to 30 keV.

3. Event 1 on 24 September 2003

[6] Figure 1 shows harmonic waves observed by the FGM instrument and simultaneous suprathermal electron and proton data from the PEACE and CIS CODIF instruments, respectively, from 0800 to 1000 UT 24 September 2003. During this interval the Cluster spacecraft were north of the plasma sheet, moving tailward and southward toward the CPS. This interval, at the end of the main phase of a minor geomagnetic storm (minimum Dst = −59), was geomagnetically active, with the AE index between 200 and 300, and Kp = 5.

[7] Figures 1a–1c show Fourier spectrograms of the B field in mean field-aligned coordinates, for which Bz points along the background field, Bx points away from the central plasma sheet (north-south), and By completes a right-handed system, pointing azimuthally eastward. Harmonic waves, with a weak fundamental near 0.8 Hz, are most evident in the Bx component because of its low background noise level, but are evident in all three components. A relatively sustained interval of such waves occurred between 0912 and 0932 UT, and shorter bursts of waves appeared at approximately 0803, 0825, 0835, 0857, and 0935 UT. Although these short intervals could be construed as evidence for temporal variations in wave generation, they are more likely spatial artifacts caused by the commonly observed flapping and kink-like motions of the magnetotail [e.g., *Grigorenko et al.*, 2007], consistent with the simultaneous changes in ion and electron fluxes from PSBL to lobe-like values noted below.

[8] The harmonic waves had considerably more power in components transverse to **B** than in the component parallel to **B**. The transverse components showed variable ellipticity (either left-hand or right-hand polarized), but were mostly linear (not shown). As *Denton et al.* [2010] point out, however, a detailed analysis suggests that the ellipticity varied on a timescale of ~5 s, so the linear polarization, based on Fourier analysis, might be an artifact of the superposition of multiple wave packets [*Denton et al.*, 1996].

[9] Omnidirectional fluxes of suprathermal electrons, shown in energy spectrogram format in Figure 1d, were greatly enhanced from ~0803 to 0836, from 0856 to 0858, and from 0911 to 0935, with center energies ranging from ~3 keV near 0803 to 1 keV from 0912 to 0932 UT. Electron fluxes were enhanced during all the times harmonic waves were observed, but the converse was not true: waves did not appear during all times of enhanced electron fluxes (e.g., near 0832 UT). Intervals of dramatically lower fluxes of ~keV electrons and simultaneous dropouts of energetic ions (Figure 1f), are evidence of transitions into the lobe region.

[10] Proton densities, shown in Figure 1e, were at or above ~0.2 cm^{-3} during each of the wave intervals, but dropped to values below 0.02 in the lobes. Densities of heavier ions (He^+, He^{++}, and O^+, not shown) were less than 10% of the proton density. Increased proton density alone was evidently also not a sufficient condition for wave occurrence. Near 0818 and between 0827 and 0834, when no waves were observed, proton densities were also at or above ~0.2 cm^{-3}. The proton energy spectrogram (Figure 1f) shows that during these latter times the energy of maximum proton flux was reduced by factors of 2 or more, from ~10 keV to ≤5 keV, and the proton pitch angle spectrogram (Figure 1g) shows that during these times the proton flux distribution shifted from pitch angles with greatest flux near 0° and 180° (bidirectional streaming) to more isotropic or unidirectional states.

4. Event 2 on 9 September 2003

[11] Figure 2, which shows similar data from 0100 to 0200 UT 9 September 2003, displays two intervals with four or even more harmonics, including a strong fundamental

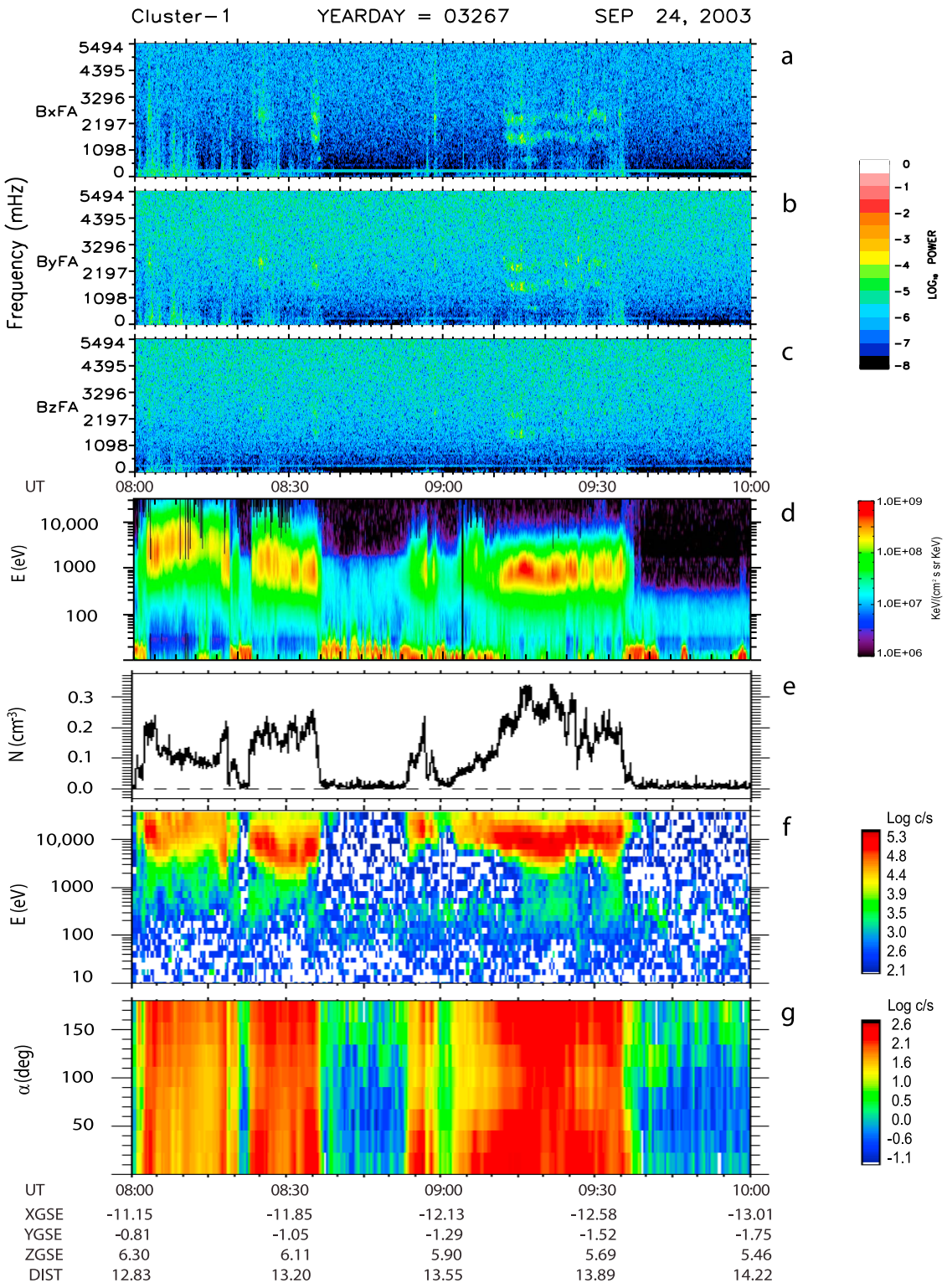

Figure 1. (a–c) Harmonic waves and (d) associated electron and (e–g) proton data observed on Cluster-1 from 0800 to 1000 UT 24 September 2003. Figures 1a–1c are differenced Fourier spectrograms of FGM magnetic field data in a mean field-aligned coordinate system. Figure 1d is an energy spectrogram of omnidirectional fluxes of electrons measured by the PEACE instrument. Figure 1e shows the proton density measured by the CIS CODIF instrument, and Figures 1f and 1g show energy and pitch angle spectrograms, respectively, of proton flux, in counts per second.

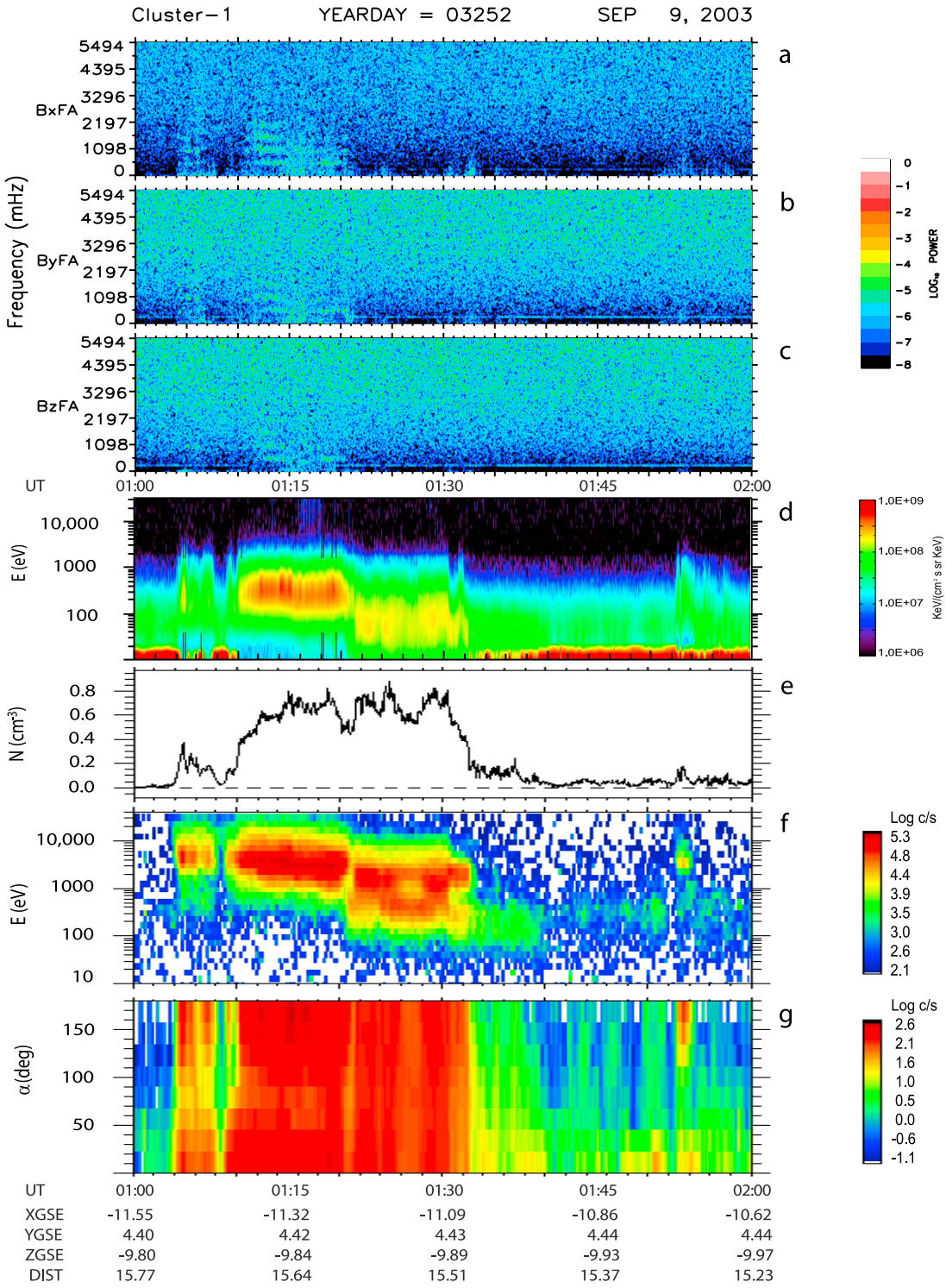

Figure 2. (a–c) Harmonic waves and (d) associated electron and (e–g) proton data, as in Figure 1, observed on Cluster-1 from 0100 to 0200 UT 9 September 2003.

(Figures 2a–2c). During this interval the Cluster spacecraft were south of the plasma sheet, moving sunward and southward from the CPS. This interval was geomagnetically quiet, with Dst ~10, AE < 100, and Kp = 2. A short burst of waves from ~0104 to 0107 UT (Figures 2a–2c) was associated with intense electron fluxes with center energy near 300 eV (Figure 2d), proton densities above 0.2 cm^{-3} (Figure 2e), proton energies averaging near 5 keV (Figure 2f), and bidirectionally streaming proton fluxes with a clear minimum near 90° pitch angle (Figure 2g). The duration of wave activity matched that of the enhancement of suprathermal proton fluxes shown in Figure 2f, but was much longer than the brief (~1 min) duration of the highest (red color) electron fluxes.

Table 1. Electron and Ion Beta Values (Particle Energy Density/Magnetic Energy Density) at Selected Times During the Events Shown in Figures 1 and 2

	0905 UT	0915 UT	0925 UT	0930 UT	0933 UT
		24 September 2003, 03267			
Waves?	N	Y	Y	Y	N
β_e	0.01	0.04	0.03	0.02	0.03
β_i	0.08	0.32	0.32	0.20	0.20
β_i/β_e	8.0	8.0	10.7	10.0	6.7
	0112 UT	0118 UT	0128 UT		
		9 September 2003, 03252			
Waves?	Y	Y	N		
β_e	0.05	0.05	0.02		
β_i	0.44	0.46	0.18		
β_i/β_e	8.8	9.2	9.0		

[12] A second, longer interval of wave activity from ~0111 to 0121 UT was associated with sharply increased fluxes of electrons and protons and again bidirectionally streaming proton fluxes. During this interval proton densities exceeded 0.4 cm^{-3}, center proton energy fell gradually from ~4 keV to ~3 keV, and center electron energy fell slightly, from ~300 to ~250 eV. Densities of heavier ions were again less than 10% of the proton density. Wave activity stopped abruptly at 0121 UT, even though proton densities continued at high levels from 0121 to ~0132 UT. During this latter interval the center proton and electron energies were both reduced by a factor of 2 or more, and the pitch angle distribution was much more isotropic. Note that the energy of the peak proton flux on this day was lower than on 24 September 2003, but the proton densities themselves were higher (0.4–0.8 cm^{-3} for 9 September versus 0.2–0.3 cm^{-3} for 24 September).

[13] Table 1 lists the values of the proton and electron beta for selected times during each of these intervals. During both wave events the ratio of proton beta to electron beta was ~9:1, but was similar during adjacent times when no waves were observed. Although there was a minimum threshold for the proton beta in these two examples (no waves appeared when $\beta_i < 0.2$), the very similar β_i and β_e values at 0930 and 0933 UT, when waves were and were not observed, respectively, indicate that either this threshold is very sensitive or that other factors may also play a role in governing the generation of these waves. As will be shown in Table 2 below, none of the waves in our data set were observed with β_i values below 0.1.

5. Statistical Study

[14] In order to identify harmonic wave events in the Cluster FGM data, Fourier spectrograms of FGM data (such as those in Figures 1a–1c) were produced for each of the four Cluster spacecraft for each 2 h interval from 1 July through 1 November 2003. Wave events were visually identified from these spectrograms, and the frequency of the fundamental wave mode was measured (or inferred, in cases when only higher multiple harmonics were evident, assuming that the fundamental frequency was equal to the difference in harmonic frequencies). It was quite typical to see 2 or 3 harmonics, distinct bands of increased magnetic activity occurring at regular frequency intervals, though as many as 4 or 5 distinct harmonics were not uncommon.

[15] From the first observed event (22 July) to the last (28 October), 13 of Cluster's 42 tail passes held at least one event. The events ranged in duration from approximately 1 min up to 50 min, with the majority of the events being under 10 min and with a median duration of 6 min.

[16] Summary plots of CIS CODIF ion data, PEACE electron data, and FGM magnetic field data were used to determine ion and electron density, energy of the peak count rate, and ion beta for each event. CIS data were obtained from Cluster 1 for most events, but during the interval from day 224 through day 235 Cluster 1 data were unavailable, and Cluster 4 data were used instead. Comparison of CIS data during events when both Cluster 1 and Cluster 4 data were available indicated very similar values, with no systematic disagreement in calibration. PEACE data, from Cluster 1, showed that the electron β was consistently ~9 times lower than the ion beta. Although this parameter was not determined for all events, this ratio is roughly consistent with the Geotail CPS data set used by *Tsyganenko and Mukai* [2003], who noted that the electron pressure was on average between 10% and 20% of the ion pressure.

5.1. Locations and Geophysical Conditions

[17] Figure 3 (left), based on data from the NASA SSCweb utility (http://sscweb.gsfc.nasa.gov/cgi-bin/sscweb/Locator_graphics.cgi), shows the GSE X and Y components of the tail-sweeping orbit of the Cluster satellites during the 4 month interval studied, 1 July to 1 November 2003. The X_{GSE} and Y_{GSE} positions of the multiple harmonic wave events identified in this study are shown in Figure 3 (right). Figure 4 (left), similarly, shows the GSE X and Z components of the Cluster orbit during this interval, and Figure 4 (right) shows the X_{GSE} and Z_{GSE} positions of these same wave events. In both Figures 3 (right) and 4 (right), events with durations under 5 min have been extended to 5 min on the plot to make them more visible.

[18] As Figures 3 (right) and 4 (right) show, all harmonic wave events were observed in the tail, one at $X_{GSE} = -4\ R_E$, and the others relatively evenly distributed in X_{GSE} from $-7\ R_E$ out to near the Cluster apogee at $\sim -19\ R_E$. Figure 3 (right) shows that they were also relatively evenly distributed in Y_{GSE} between +8 and $-9\ R_E$, but with two dawnside events beyond $Y_{GSE} = +10$. Figure 4 (right) reveals that no harmonic events were observed for $|Z_{GSE}| < 3\ R_E$. Comparison of Figures 4 (left) and 4 (right) shows that although the absence of low-Z_{GSE} events is partly an artifact of the Cluster orbit, their absence near apogee cannot be explained in this way. The distribution, however, is consistent with the fact that each of these harmonic wave events occurred in the plasma sheet

Table 2. Values of Plasma Parameters During Harmonic ULF Wave Events in This Study

Parameter	Average	Standard Deviation	Minimum	Maximum
Ion density (cm^{-3})	0.20	0.09	0.1	0.6
Ion energy (keV)	10.2	5.3	3	30
Ion pressure (nPa)	0.29	0.08	0.09	0.43
Ion beta	0.40	0.23	0.10	1.1

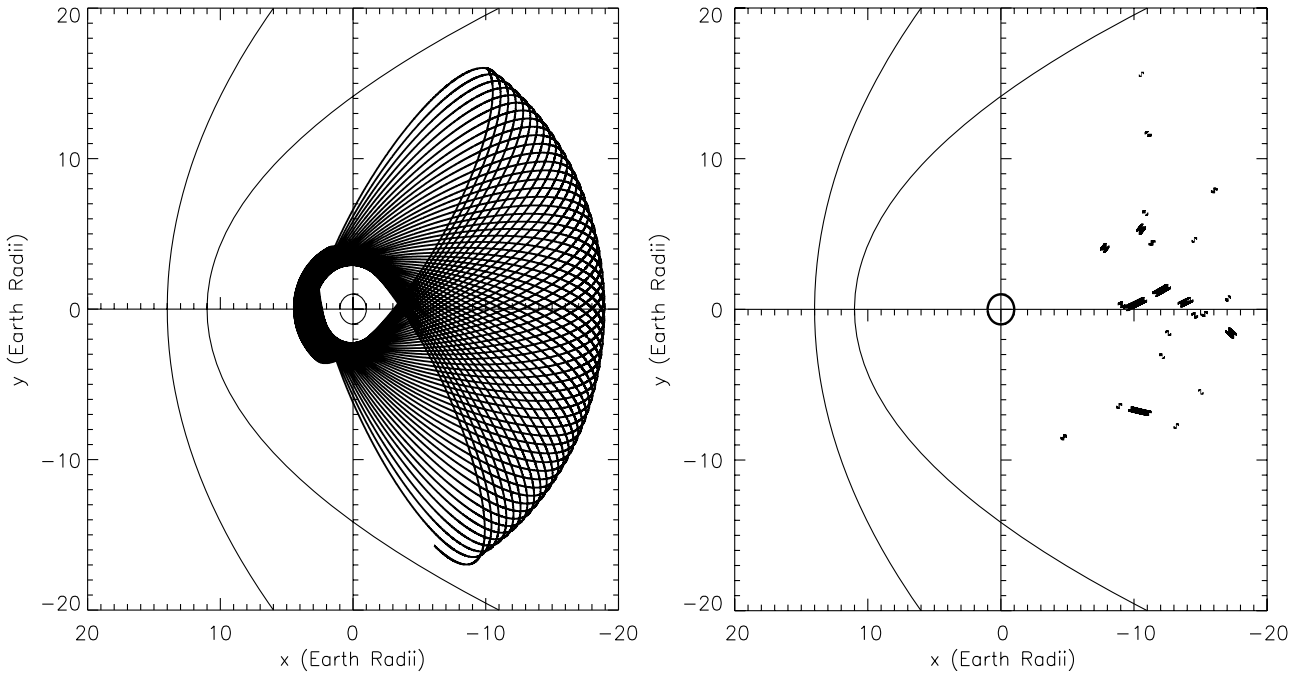

Figure 3. (left) Plot of the GSE X and Y components of the orbit of the Cluster satellites during the 4 month interval from 1 July to 1 November 2003. (right) Plot of the X_{GSE} and Y_{GSE} positions of the multiple harmonic wave events identified in this study. Events with durations under 5 min have been extended to 5 min on the plot to make them more visible.

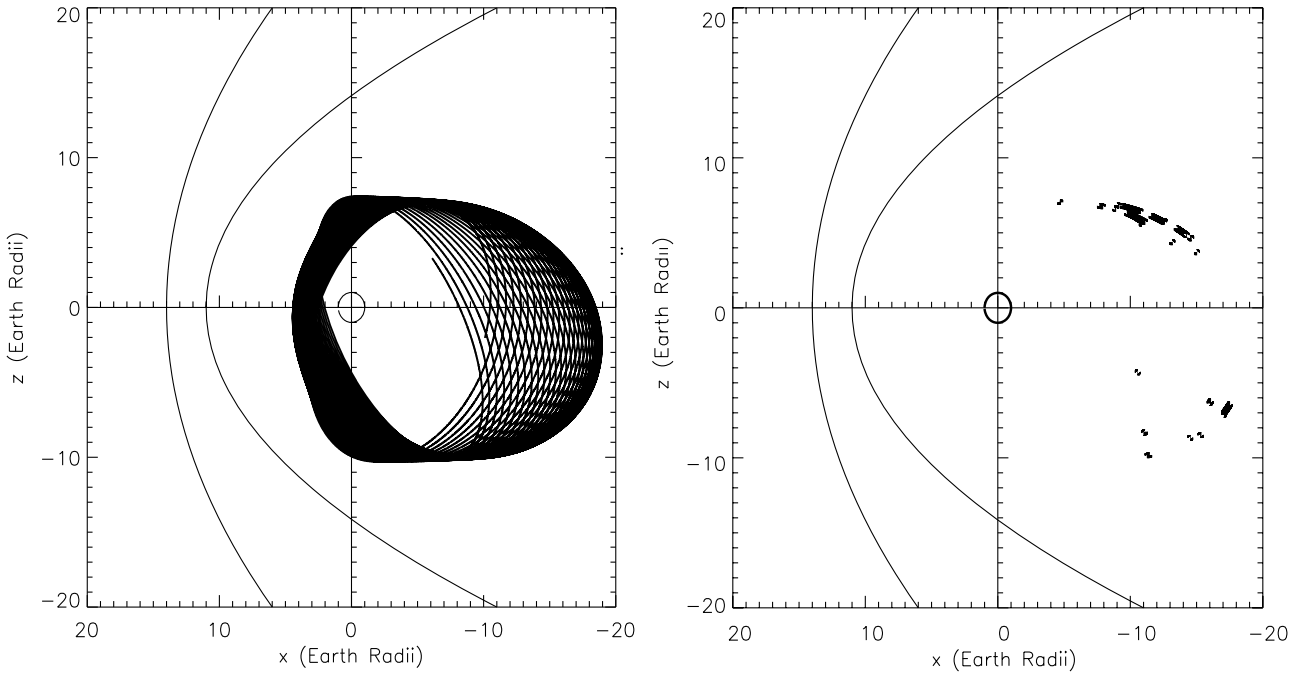

Figure 4. (left) Plot of the GSE X and Z components of the orbit of the Cluster satellites during the 4 month interval from 1 July to 1 November 2003. (right) Plot of the X_{GSE} and Z_{GSE} positions of the multiple harmonic wave events identified in this study. Events with durations under 5 min have been extended to 5 min on the plot to make them more visible.

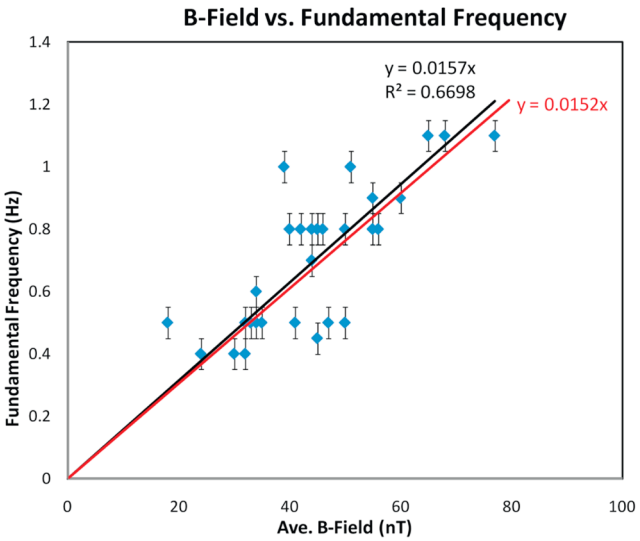

Figure 5. Plot of the frequency of the fundamental of each multiple-harmonic event included in this study, as a function of the magnitude of the simultaneously observed magnetic field, **B**. The black line shows a least squares best fit through zero, and the red line indicates the proton gyrofrequency, Ω_{cp}, at the given **B** value.

boundary layer, and none in the central plasma sheet. More and longer-duration events were observed north of the Z_{GSE} = 0 plane than south of it, but they were more localized: in the north Z_{GSE} positions ranged from +3 to +7 R_E, and in the south, from −3 to −10 R_E. Their spatial pattern appears to be largely an artifact of the Cluster orbits during this interval.

[19] Examination of the Dst, Kp, and AE indices for all events (not shown) revealed little evidence of correlation between wave occurrence and level of geomagnetic disturbance, and no simple relation between event location and any of these indices. This negative result is consistent with the observations of two earlier studies. *Eastman et al.* [1984, 1985] noted that PSBL signatures, including counterstreaming ion flow, occurred at all conditions of geomagnetic activity, including extended quiet periods, and *Baumjohann et al.* [1988] found that the ion population in the PSBL was less affected by substorm activity than the central plasma sheet ions.

5.2. Magnetic Field and Plasma Conditions

[20] Figure 5 shows the dependence of the fundamental frequency of the multiple harmonic waves, as determined from Fourier spectrograms such as those in Figures 1 and 2, on the magnitude of the simultaneously observed local magnetic field, **B**. The black line shows a least squares best fit line through zero, with linear correlation coefficient R^2 = 0.67, and the red line indicates the proton gyrofrequency, Ω_{cp}, at the given **B** value. The close agreement in slopes (6% difference) between the line fit to the observed wave fundamental frequencies and Ω_{cp} suggests that most or all of these waves were observed near the region of their generation, rather than nearer Earth or deeper down the tail. This further suggests that these waves do not propagate far along magnetic field lines, consistent with their never yet having been observed in ground data.

[21] Table 2 shows the distributions of values of ion density, energy of peak ion count rate ("ion energy"), ion pressure, and ion beta for the 35 harmonic wave events. All values had substantial variations, with standard deviations of the distributions roughly half the average value for ion density, ion energy, and ion beta; only the ion pressure exhibited a smaller variation.

[22] Figure 6 shows normalized occurrence distributions of ion energy (Figure 6a), ion density (Figure 6b), ion beta, the ratio of ion pressure to magnetic pressure (Figure 6c), and ion pressure (Figure 6d), during the 35 harmonic wave events in this study (solid line) and immediately before and after each event (dashed line). Occurrence rates were calculated for 5 bins per decade, and displayed such that the horizontal value of each point is at the center of a bin. The ion energy distribution during wave events differed only slightly from that observed before and after wave events (Figure 6a), suggesting that ion energy alone is not a critical factor for wave growth. The distributions for the other three

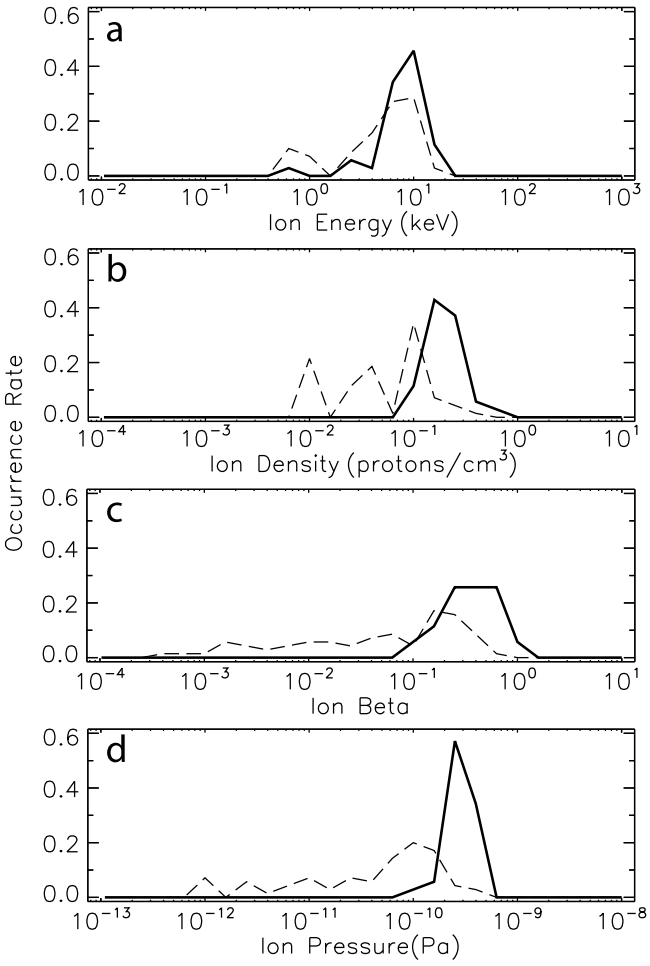

Figure 6. Normalized occurrence distributions of selected plasma parameters during the 35 harmonic wave events in this study (solid line) and immediately before and after each event (dashed line). (a) Ion energy, (b) ion density, (c) ion beta, and (d) ion pressure.

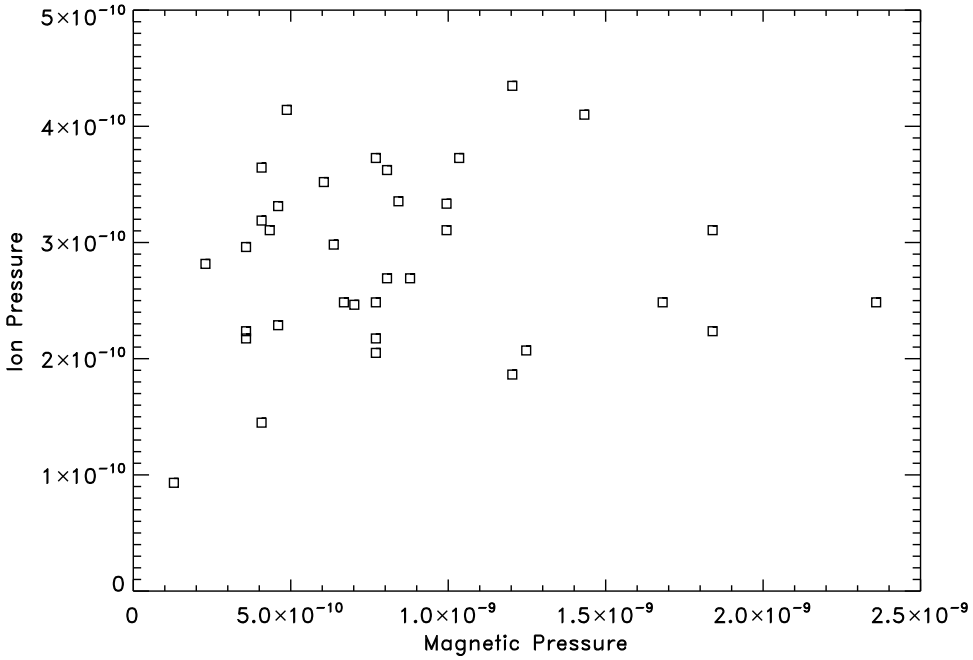

Figure 7. Plot of ion pressure versus magnetic pressure for the events in this study.

panels were significantly different for wave events than temporally adjacent nonwave intervals. Each wave interval distribution had a sharp lower bound that was above many of the nonwave interval values, but in no case was there a clear threshold above which waves would always be present. The ion density distribution during wave events (Figure 6b) had a width similar to that of the ion energy, but the density was generally higher during wave events. The ion beta distribution during wave events (Figure 6c) was somewhat wider, and there was more overlap between beta values during intervals with and without wave activity. The ion pressure (Figure 6d) was the most sharply peaked of the four parameters shown in Figure 6, and showed the most difference from the distribution during nonwave intervals.

[23] Figure 7, a scatterplot of ion pressure versus magnetic pressure ($B^2/2\mu_0$) during each wave event, shows essentially no correlation. That is, over a wide range of values of magnetic pressure (a factor of over 18), the ion pressure showed no clear trend. 33 of the 35 wave events had ion pressures between 0.15 and 0.45 nPa, and only 2 intervals with no wave activity (see Figure 6) had pressure values (0.33 and 0.46 nPa) above the 0.29 nPa average value during wave intervals. Because beta is defined as the ratio of these two pressures, the range of beta values can thus be expected to be larger than the range of ion pressures, consistent with Figure 6, and the much tighter distribution of ion pressures suggests that this parameter may be the more important factor determining wave instability.

[24] In Table 3 we compare the average values of plasma parameters during these wave intervals to values found in earlier studies in the tail region using AMPTE IRM satellite data [*Baumjohann et al.*, 1988, 1989] and Geotail data [*Tsyganenko and Mukai*, 2003]. The average ion density, ion temperature, ion pressure, and ion beta during these wave events were all larger than the PSBL averages compiled by *Baumjohann et al.* [1988], and three of the four (ion temperature, ion pressure, and ion beta) were even larger than values they found in the outer CPS region [*Baumjohann et al.*, 1989]. However, the variance in the values noted by *Baumjohann et al.* [1988] was also quite large (see their Figure 7, in which the error bars drawn represent only 1/5 of the variance). In particular, the average ion density during wave events in 2003 was roughly a factor of 2 larger than the corresponding averages in the 1986 *Baumjohann et al.* [1988] PSBL data set. The average ion temperature, pressure, and ion beta values showed an even larger increase. The average ion beta exceeded the 1986 PSBL average by a factor of 8–20, and in every case ion beta values during the

Table 3. Average Plasma Parameters During the 35 Harmonic ULF Wave Events in This Study, and Values Based on Observations by *Baumjohann et al.* [1988, 1989] in the PSBL, Outer CPS, and Inner CPS, and by *Tsyganenko and Mukai* [2003] in the CPS

Quantity	Wave Events	*Baumjohann et al.* [1988, 1989] PSBL	*Baumjohann et al.* [1988, 1989] Outer CPS	*Baumjohann et al.* [1988, 1989] Inner CPS	*Tsyganenko and Mukai* [2003] CPS
Ion density	0.20 cm^{-3}	0.08–0.15 cm^{-3}	0.4 cm^{-3}	0.5 cm^{-3}	0.625 cm^{-3}
Ion temperature	10.2 keV	1.7–4.5 keV	3.9 keV	6.5 keV	3.795 keV
Ion pressure	0.29 nPa	0.014–0.07 nPa	0.17 nPa	0.35 nPa	0.229 nPa
Ion beta	0.40	0.02–0.05	0.3	3–30	13 (median)

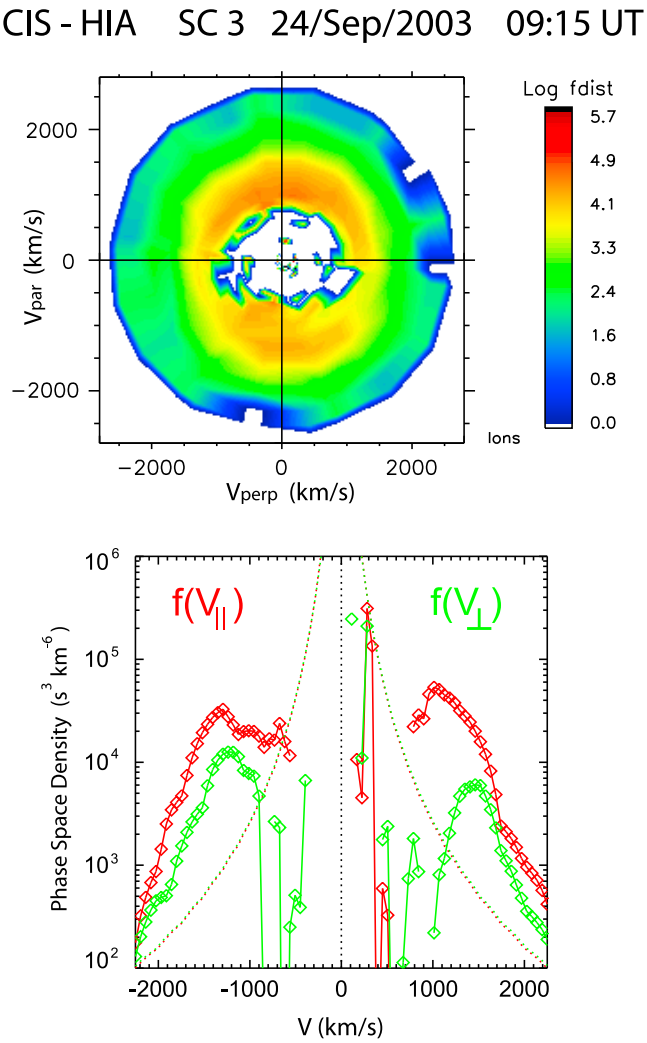

Figure 8. (top) Color-coded two-dimensional cut of the ion distribution function, and (bottom) one-dimensional cuts of the ion phase space distribution function versus energy parallel to the magnetic field (red) and perpendicular to the magnetic field (green), observed by the CIS-HIA instrument on Cluster 3 during a 4 s interval (one spin period) beginning at 0915:05.401 UT 24 September 2003. The dashed lines are one-count levels, so values below these lines are not reliable.

wave events in 2003 exceeded the upper 1986 PSBL average of 0.05. However, the average ion beta value during these wave events was still substantially below the average of values found in the inner CPS by *Baumjohann et al.* [1989] and the median CPS beta value of *Tsyganenko and Mukai* [2003], and the average ion pressure during wave events was also comparable to the corresponding CPS values.

[25] We remind readers that in every case the harmonic waves were associated with counterstreaming, ring-type ion distributions that are characteristic of the PSBL, not the CPS. Although the data used in the *Baumjohann et al.* [1988, 1989] studies are from 1986 (during solar minimum), the data from November 1994 to April 1998 used in the *Tsyganenko and Mukai* [2003] study are from conditions comparable to those in this study, namely, during the declining phase of the solar cycle. Hence, because of the reasonably good agreement between these two earlier data sets in the CPS region, we believe the comparisons shown in Table 3 suggest that these waves are associated with higher than usual levels of these ion parameters in the PSBL.

5.3. Suprathermal Particle Distributions

[26] Figures 1 and 2 showed evidence that anisotropic proton distributions were associated with these harmonic waves. In this section we present a more detailed look at the velocity distributions of both ions and electrons during short intervals on each of these days. In Figures 8–11 we show color-coded pitch angle distributions and cuts of particle

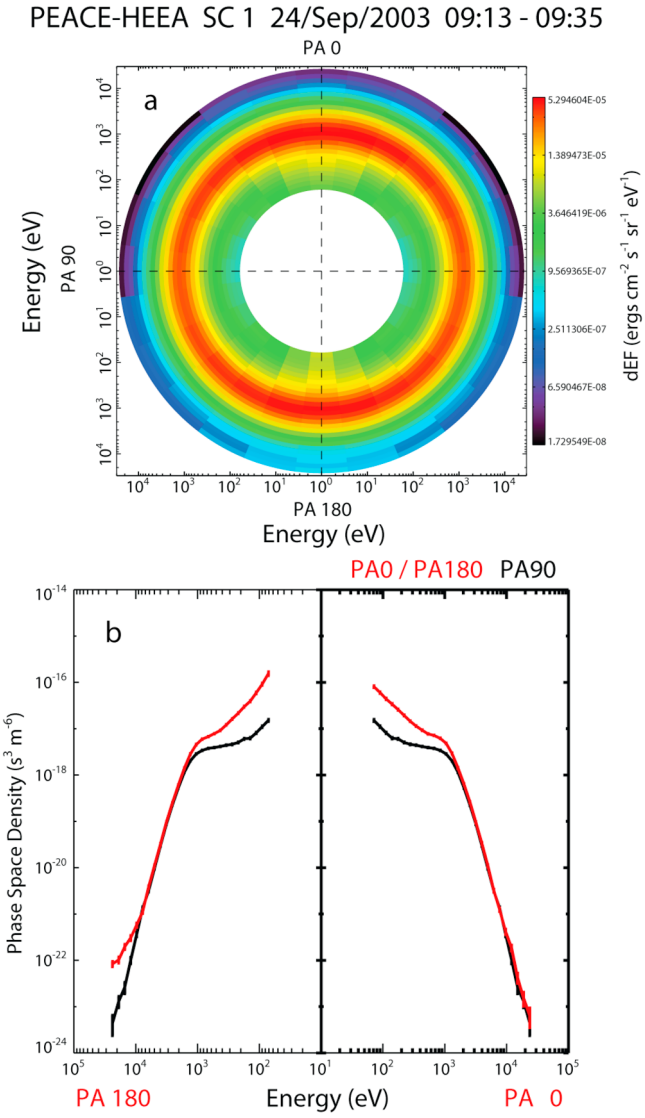

Figure 9. (a) Color-coded electron pitch angle distributions of the differential energy flux of electrons, and (b) cuts of electron phase space density versus energy parallel, antiparallel, and perpendicular to the magnetic field, observed by the PEACE HEEA instrument on Cluster 1 between 0913 and 0934 UT 24 September 2003.

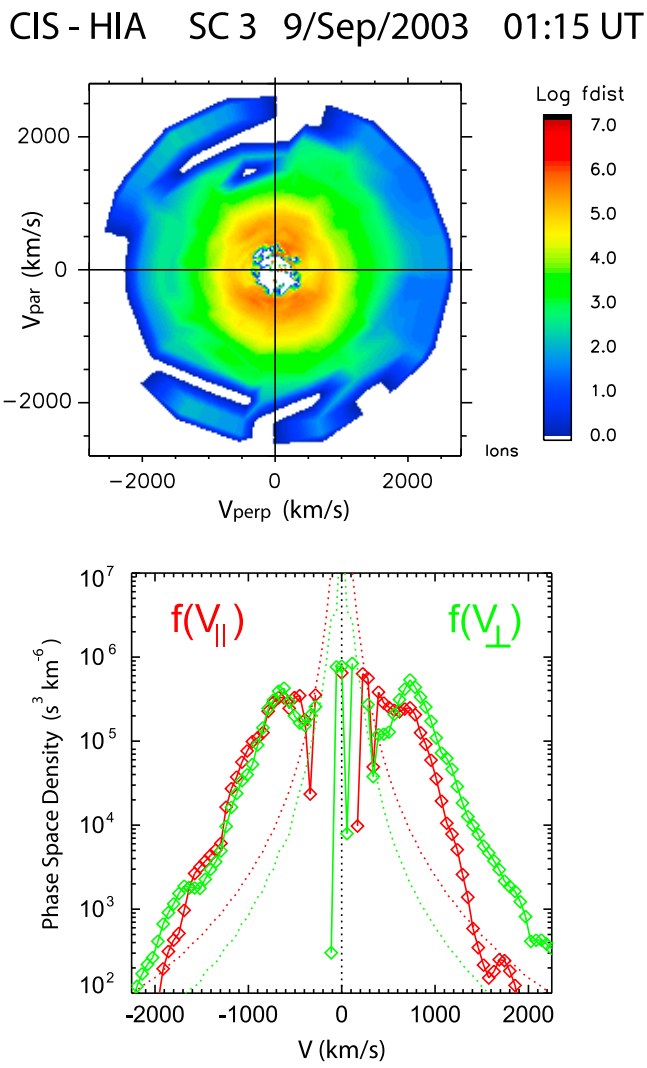

Figure 10. (top) Color-coded two-dimensional cut of the ion distribution function, and (bottom) one-dimensional cuts of the ion phase space distribution function versus energy parallel to the magnetic field (red) and perpendicular to the magnetic field (green), observed by the CIS-HIA instrument on Cluster 3 during a 4 s interval beginning at 0115:04.551 UT 9 September 2003. The dashed lines are one-count levels, so values below these lines are not reliable.

energy flux or phase space densities versus energy parallel, antiparallel, and perpendicular to the magnetic field.

[27] The ion velocity distribution shown in Figure 8 (top), obtained by the CIS/HIA instrument over a 4 s interval (one spin period) beginning at 0915:05 UT 24 September, shows count rate maxima near 1300 m/s both parallel (upward, pitch angle = 0°) and antiparallel (downward, pitch angle = 180°) to **B**, and decreasing counts away from these directions. Figure 8 (bottom), showing cuts of the phase space distribution function again parallel and perpendicular to **B**, indicates more quantitatively that more ions were moving along **B** than opposite to it, while the perpendicular flux (pitch angle = 90°) was considerably lower over a wide range of energies. The 24 September 2003 event occurred while Cluster was north of the CPS, so **B** was directed earthward. This means that the largest fluxes of ions were directed earthward.

[28] The distribution shown in Figure 8 can be described as intermediate between a counterstreaming beam distribution and a ring-type distribution. Although the fluxes parallel and antiparallel to **B** greatly exceeded those in the perpendicular direction, the largest fluxes are not narrowly confined near 0° and 180° pitch angle, and there is significant flux at all pitch angles at ion speeds near 1300 m/s. Very similar ion distributions in the PSBL, obtained by the ISEE 2 Fast Plasma Experiment, were reported by *Onsager et al.* [1991].

[29] The electron data for this event shown in Figure 9a, extending from 0913 to 0935 UT, are displayed in a format similar to that of Figure 8 (top) except that the color scale shows differential energy flux rather than count rates. The

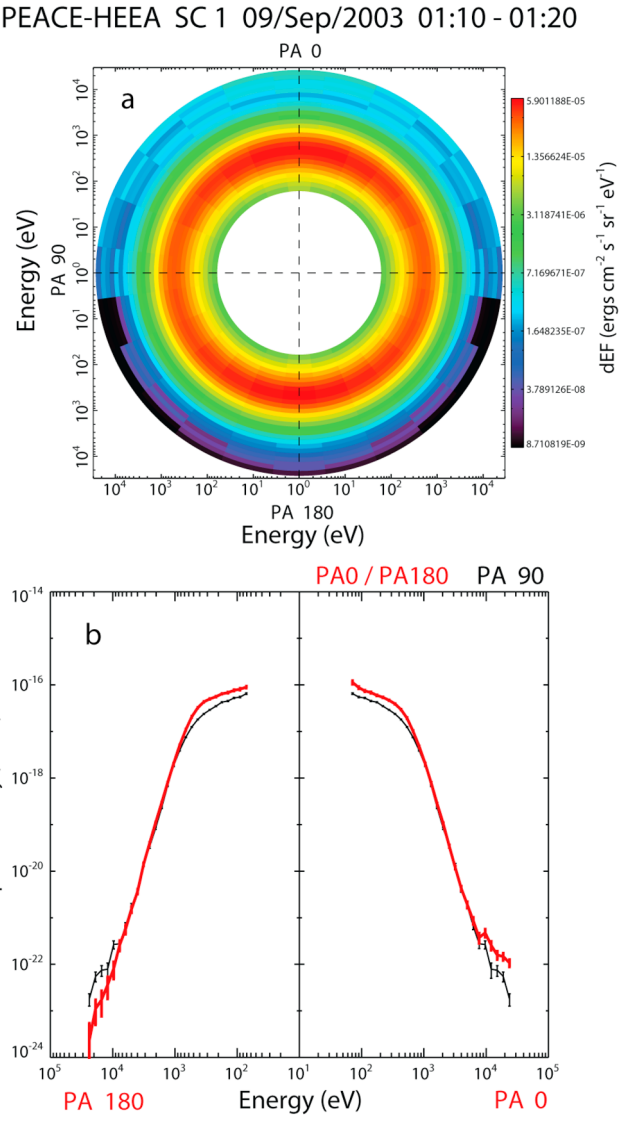

Figure 11. (a) Color-coded electron pitch angle distributions, and (b) cuts of electron phase space density versus energy parallel, antiparallel, and perpendicular to the magnetic field, observed by the PEACE HEEA instrument on Cluster 1 between 0110 and 0120 UT 9 September 2003.

electron distribution, averaged over the interval, was much more isotropic in pitch angle than the proton distribution, but also showed a decline in flux below a maximum near 1.2 keV. This decline, however, is an artifact of the data being plotted in differential energy flux form. Cuts in phase space density, shown in Figure 9b, indicate an inflection point near 1.2 keV rather than a maximum. Figure 9b is consistent with Figure 9a in showing that the distribution was nearly isotropic from 1.2 keV to ~8 keV, and that there were more electrons in the parallel and antiparallel directions than the perpendicular direction at energies below 1.2 keV. Although the phase space densities slightly below 1.2 keV were roughly equal at pitch angles of 0° and 180°, at energies both much below this value and above ~8 keV fluxes were larger at 180° pitch angle, thus with a larger fraction of electrons appearing to flow tailward. This is in fact an instrumental effect caused at higher energies by sunlight entering the instrument aperture and at lower energies by the presence of a larger number of spacecraft photoelectrons on the sunlit side of the spacecraft.

[30] Similar patterns were found for both ion and electron distributions for the 9 September event, although both electron and ion energies were lower on this day and peak fluxes were higher (consistent with Figures 1 and 2), and the ion distribution was more ring-like. During this event the Cluster spacecraft were south of the CPS, so **B** was directed tailward. The ion data (Figure 10, top), obtained over a 4 s interval beginning at 0115:04 UT, showed larger fluxes antiparallel to **B** (again earthward). During this event the phase space cuts parallel and perpendicular to **B** (Figure 10, bottom) show roughly similar fluxes, but Figure 10 (top) shows that when all pitch angles are considered, there were again greater fluxes parallel/antiparallel to **B** than perpendicular to it. The electron distribution (Figure 11) was again nearly isotropic at energies above the flux peak. On this day there was much less enhancement in field-aligned phase space density below 500 eV. There was again an instrument-caused enhancement above ~8 keV in the tailward electron flux (at 0° pitch angle during this event) due to sunlight.

[31] These same flux patterns were characteristic of the set of 35 wave events, and are consistent with the earlier observations of *Parks et al.* [1998] that counterstreaming electrons occur in the same regions where earthward and tailward streaming ion beams are observed. The ion flux was peaked in the parallel and antiparallel directions, and more ions streamed earthward. The electron flux was more modestly peaked in these directions; on average bidirectional fluxes of electrons were present when the Pc1 waves were present, and they extended down to lower energies than the perpendicular particle population. The pattern was the same for events both north and south of the midtail.

6. Discussion and Summary

[32] Several studies have reported that when passing from the PSBL to the CPS the ion distribution changes from two crescent-shaped distributions in velocity space, to a ring-shaped distribution, and ultimately to an isotropic hot proton distribution [e.g., *Gary and Winske*, 1990; *Onsager et al.*, 1991] (and others reviewed by *Broughton et al.* [2008]). Wave activity has often been suggested as the agent responsible for these transitions, and the harmonic waves reported in this study show a close observational link to this transition. We note, however, that *Onsager et al.* [1991] used a modeled reconnection source in the distant tail and time of flight effects to reproduce the observed transition in ion and electron distributions without recourse to waves. We stress that multiple-harmonic waves are not at all rare in the Cluster data set. They were observed on 31% (13 of 42) of the tail passes during 2003. Figure 3 suggests that the fraction of passes with harmonic waves was even greater near midnight; indeed, during the 21 day period when Cluster's apogee was closest to 0 MLT (28 August to 17 September 2003), such waves were observed during 5 of the 8 tail passes.

[33] In addition to the observation that, as in earlier reports, multiple-harmonic waves occurred only in the PSBL, we have noted that all of the wave events had an observed or inferred fundamental frequency near the local proton cyclotron frequency Ω_{cp}, suggesting observation near the region of their generation, and consistent with the earlier wave telescope observations of *Broughton et al.* [2008] showing **k** perpendicular to **B**. We are, however, not able to duplicate the wave telescope analysis to determine **k** for each of these events. Only two of the 35 events included in this study were found by *Broughton et al.* [2008] to have a spatial configuration optimal for wave telescope analysis; that is, the maximum separation between any two spacecraft was under 1000 km, and the spacecraft configuration was close to that of an ideal tetrahedron. Minimum variance techniques provide an alternate means to determine the direction of wave propagation, but the observations analyzed by *Denton et al.* [2010] suggest the likelihood of superposition of wave packets, which compromises the effectiveness of this technique as well. Although we are thus unable to confirm that each of the events in this survey shared the wave propagation characteristics of the three events studied by Broughton *et al.*, we note that two of these 35 events were shown by Broughton *et al.* to have **k** perpendicular to **B**, and these events did not differ in any way from the others in our data set. It thus is reasonable to associate these waves with the simultaneous, locally observed ion and electron distributions, and to consider their possible role in generating these waves, which in turn would isotropize these particle distributions.

[34] Both the two example events and the comparisons of ion density, ion beta, and values before, during, and after wave intervals in Figure 6 shows that multiple-harmonic waves appeared only during times of elevated ion (and usually electron) densities and especially elevated beta values. Waves were associated with counterstreaming ion beams (greater fluxes parallel and antiparallel to B than perpendicular), and did not occur when the ions were isotropically distributed in pitch angle. In addition, ion distributions exhibited a shell-like or ring-like character: relatively few ions were observed at energies significantly lower than the observed flux peaks, so in this region, the slope of the distribution function, $\partial f/\partial v$, is >0. This suggests that these waves, and also the other varieties of waves observed in the PSBL such as broadband electrostatic noise [*Grabbe and Eastman*, 1984], may be associated with particular stages of the presumed progression of particle distributions. Indeed, the theoretical analysis of *Grabbe and Eastman* [1984] suggested that broadband electrostatic noise in the PSBL serves to pitch angle scatter the

ion beams, while the analysis of *Denton et al.* [2010], using data from the event shown in Figure 2, suggested that it is the shell-like or ring-like character of the distributions, rather than their beam-like anisotropy, that is unstable to the harmonic electromagnetic wave modes that are the focus of this study.

[35] The elevated values of ion plasma parameters during these wave events compared to typical PSBL values is consistent with the harmonic waves being found either closer to the CPS than the lobe, or being generated during times when the plasma parameters are elevated throughout the magnetotail. The lack of any statistical association of these wave events with increased magnetic activity favors the first interpretation, although direct verification of such a location is beyond the scope of this study.

[36] Although our finding that the occurrence of harmonic waves is associated in every case with counterstreaming ion fluxes might suggest that the beam-like character of the ion distributions rather than their shell-like character is responsible for wave growth, this association may instead reflect either the overlapping character of the regions of the PSBL that are unstable to different wave modes, or simply the necessity of replenishing the unstable distributions needed for local generation. Theoretical analysis using numerical simulations may provide a means to reconcile this apparent contradiction.

[37] As noted in section 5.2, analysis of the ion plasma parameters during the 35 wave events showed apparent thresholds for wave occurrence in both ion number density and ion beta. The sharpest boundary for wave events appeared to involve the ion pressure (Figure 6d). This may suggest a "flute-like" instability with wave vector and velocity perturbations perpendicular to the background magnetic field, so that the magnetic field is affected minimally by the oscillations. There was no sharp boundary in ion beta for the wave events, and sometimes periods of time without waves had values of ion beta that at other times were associated with waves. These facts suggest that the instability responsible for these waves is sensitive to the detailed velocity space distribution. *Denton et al.* [2010] found that a flute-like instability driven by a ring-like velocity space distribution function persists over a wide range of beta values (although the character of the instability changes with the plasma beta). But the largest theoretical growth rate normalized to the proton cyclotron frequency occurred for ion beta equal to 0.40. This is also the average ion beta value found for the observed wave events (Table 2).

[38] It is our hope that, by using the occurrence data reported here, it will be possible to estimate whether the occurrence of the harmonic waves described in this study and by *Denton et al.* [2010] is sufficient to account for the isotropization of the beams seen at the edge of the PSBL.

[39] **Acknowledgments.** The work of M.J.E. and M.C.B. on Cluster was initiated by grants from the German Fulbright Commission. Work at Augsburg College was supported by NSF grants ATM-0827903 and ANT-0538379. Work at Dartmouth College was supported by NSF grants ANT-0538379 and ATM-0120950 (Center for Integrated Space Weather Modeling, CISM, funded by the NSF Science and Technology Centers Program). Work at the University of California, Berkeley, was supported by NASA grant NNX08AF29G. Work at the Technical University of Braunschweig was supported by the German Bundesministerium für Wirtschaft und Technologie and the Deutsche Zentrum für Luft- und Raumfahrt. Work at UCL-MSSL was supported by UK STFC Rolling Grant PP/E/001173/1. Cluster work at CESR was funded by CNES grants.

[40] Masaki Fujimoto thanks Peter Yoon and another reviewer for their assistance in evaluating this paper.

References

Angelopoulos, V., R. C. Elphic, S. P. Gary, and C. Y. Huang (1989), Electromagnetic instabilities in the plasma sheet boundary layer, *J. Geophys. Res.*, *94*, 15,373–15,383, doi:10.1029/JA094iA11p15373.

Balogh, A., et al. (2001), The Cluster magnetic field investigation: Overview of in-flight performance and initial results, *Ann. Geophys.*, *19*, 1207–1217.

Bauer, T. M., W. Baumjohann, R. A. Treumann, N. Sckopke, and H. Lühr (1995), Low-frequency waves in the near-Earth plasma sheet, *J. Geophys. Res.*, *100*, 9605–9618, doi:10.1029/95JA00136.

Baumjohann, W., G. Paschmann, N. Sckopke, C. A. Cattell, and C. W. Carlson (1988), Average ion moments in the plasma sheet boundary layer, *J. Geophys. Res.*, *93*, 11,507–11,520.

Baumjohann, W., G. Paschmann, and C. A. Cattell (1989), Average plasma properties in the central plasma sheet, *J. Geophys. Res.*, *94*, 6597–6606.

Bogdanov, A. T., K.-H. Glassmeier, G. Musmann, M. K. Dougherty, S. Kellock, P. Slootweg, and B. Tsurutani (2003), Ion cyclotron waves in the Earth's magnetotail during CASSINI's Earth swing-by, *Ann. Geophys.*, *21*, 2043–2057.

Broughton, M. C., M. J. Engebretson, K.-H. Glassmeier, Y. Narita, A. Keiling, K.-H. Fornacon, G. K. Parks, and H. Rème (2008), Ultra-low-frequency waves and associated wave vectors observed in the plasma sheet boundary layer by Cluster, *J. Geophys. Res.*, *113*, A12217, doi:10.1029/2008JA013366.

Chaston, C. C., Y. D. Hu, B. J. Fraser, R. C. Elphic, and C. Y. Huang (1994), Electromagnetic ion cyclotron waves observed in the near Earth plasma sheet boundary layer, *J. Geomagn. Geoelectr.*, *46*, 987–995.

Chaston, C. C., J. W. Bonnell, J. P. McFadden, R. E. Ergun, and C. W. Carlson (2002), Electromagnetic ion cyclotron waves at proton cyclotron harmonics, *J. Geophys. Res.*, *107*(A11), 1351, doi:10.1029/2001JA900141.

Denton, R. E., B. J. Anderson, G. Ho, and D. C. Hamilton (1996), Effects of wave superposition on the polarization of electromagnetic ion cyclotron waves, *J. Geophys. Res.*, *101*, 24,869–24,885.

Denton, R. E., M. J. Engebretson, A. Keiling, A. P. Walsh, S. P. Gary, P. M. E. Décréau, C. A. Cattell, and H. Rème (2010), Multiple harmonic ULF waves in the plasma sheet boundary layer: Instability analysis, *J. Geophys. Res.*, *115*, A12224, doi:10.1029/2010JA015928.

Eastman, T. E., L. A. Frank, W. K. Peterson, and W. Lennartsson (1984), The plasma sheet boundary layer, *J. Geophys. Res.*, *89*, 1553–1572.

Eastman, T. E., L. A. Frank, and C. Y. Huang (1985), The boundary layers as the primary transport regions of the Earth's magnetotail, *J. Geophys. Res.*, *90*, 9541–9560.

Escoubet, C. P., M. Fehringer, and M. Goldstein (2001), The Cluster mission, *Ann. Geophys.*, *19*, 1197–1200.

Gary, S. P., and D. Winske (1990), Computer simulations of electromagnetic instabilities in the plasma sheet boundary layer, *J. Geophys. Res.*, *95*, 8085–8094, doi:10.1029/JA095iA06p08085.

Glassmeier, K.-H., et al. (2001), Cluster as a wave telescope: First results from the fluxgate magnetometer, *Ann. Geophys.*, *19*, 1439–1477.

Grabbe, C. L., and T. E. Eastman (1984), Generation of broadband electrostatic noise by ion beam instabilities in the magnetotail, *J. Geophys. Res.*, *89*, 3865–3872.

Grigorenko, E. E., J.-A. Sauvaud, and L. M. Zelenyi (2007), Spatial-temporal characteristics of ion beamlets in the plasma sheet boundary layer of magnetotail, *J. Geophys. Res.*, *112*, A05218, doi:10.1029/2006JA011986.

Johnstone, A. D., et al. (1997), PEACE: A Plasma Electron and Current Experiment, *Space Sci. Rev.*, *79*, 351–398.

Kawano, H., M. Fujimoto, T. Mukai, T. Yamamoto, T. Terasawa, Y. Saito, S. Machida, S. Kokubun, and A. Nishida (1994), Right-handed ion/ion resonant instability in the plasma sheet boundary layer: GEOTAIL observation in the distant tail, *Geophys. Res. Lett.*, *21*, 2887–2890, doi:10.1029/94GL02106.

Motschmann, U., T. Woodward, K.-H. Glassmeier, D. J. Southwood, and J. Pinçon (1996), Wavelength and direction filtering by magnetic measurements at satellite arrays: Generalized minimum variance analysis, *J. Geophys. Res.*, *101*, 4961–4966, doi:10.1029/95JA03471.

Onsager, T. G., M. F. Thomsen, R. C. Elphic, and J. T. Gosling (1991), Model of electron and ion distributions in the plasma sheet boundary layer, *J. Geophys. Res.*, *96*, 20,999–21,011.

Parks, G. K., et al. (1984), Particle and field characteristics of the high-latitude plasma sheet boundary layer, *J. Geophys. Res.*, *89*, 8885–8906.

Parks, G., L. J. Chen, M. McCarthy, D. Larson, R. P. Lin, T. Phan, H. Reme, and T. Sanderson (1998), New observations of ion beams in the plasma sheet boundary layer, *Geophys. Res. Lett.*, *25*, 3285–3288.

Parks, G. K., L. J. Chen, M. Fillingim, and M. McCarthy (2001), Kinetic characterization of plasma sheet dynamics, *Space Sci. Rev.*, *95*, 237–255.

Rème, H., et al. (2001), First multispacecraft ion measurements in and near the Earth's magnetosphere with the identical Cluster ion spectrometry (CIS) experiment, *Ann. Geophys.*, *19*, 1303–1354.

Tsurutani, B. T., and E. J. Smith (1984), Magnetosonic waves adjacent to the plasma sheet in the distant magnetotail: ISEE-3, *Geophys. Res. Lett.*, *11*, 331–334, doi:10:1029/GL011i004p03331.

Tsurutani, B. T., I. G. Richardson, R. M. Thorne, W. Butler, E. J. Smith, S. W. H. Cowley, S. P. Gary, S.-I. Akasofu, and R. D. Zwickl (1985), Observations of the right-hand resonant ion beam instability in the distant plasma sheet boundary layer, *J. Geophys. Res.*, *90*, 12,159–12,172, doi:10.1029/JA090iA12p12159.

Tsyganenko, N. A., and T. Mukai (2003), Tail plasma sheet models derived from Geotail particle data, *J. Geophys. Res.*, *108*(A3), 1136, doi:10.1029/2002JA009707.

M. C. Broughton and R. E. Denton, Department of Physics and Astronomy, Dartmouth College, Hanover, NH 03755, USA. (matthew.broughton@dartmouth.edu; richard.e.denton@dartmouth.edu)

M. J. Engebretson, C. R. G. Kahlstorf, and J. L. Posch, Department of Physics, Augsburg College, 2211 Riverside Ave., Minneapolis, MN 55454, USA. (engebret@augsburg.edu; kahlstor@augsburg.edu; posch@augsburg.edu)

K.-H. Fornaçon, Institut für Geophysik und Extraterrestrische Physik, Technische Universität Braunschweig, D-83106 Braunschweig, Germany. (k-h.fornacon@tu-bs.de)

A. Keiling, Space Sciences Laboratory, University of California, Berkeley, CA 94720-7450, USA. (keiling@ssl.berkeley.edu)

C. J. Owen and A. P. Walsh, Mullard Space Science Laboratory, University College London, Holmbury St. Mary, Dorking RH5 6NT, UK. (cjo@mssl.ucl.ac.uk; apw@mssl.ucl.ac.uk)

H. Rème, CESR, University of Toulouse, UPS, 9 ave. du Colonel Roche, F-31028 Toulouse CEDEX 4, France. (reme@cesr.fr)